ACS Sustainable Chemistry & Engineering

Research Article

pubs.acs.org/journal/ascecg

How Impurities Affect CO_2 Capture in Metal−Organic Frameworks Modified with Different Functional Groups

Jiamei Yu and Perla B. Balbuena*

Artie McFerrin Department of Chemical Engineering and Materials Science and Engineering Program, Texas A&M University, College Station, Texas 77843-3122, United States

Supporting Information

ABSTRACT: The introduction of functional groups in metal−organic frameworks (MOFs) has been found to be a successful strategy for improving CO_2 selective separation from N_2. However, little is known regarding how impurities such as H_2O and SO_2 may interfere with CO_2 capture as a function of the properties of the functional groups in MOF adsorbent materials. Here, the effects of water and SO_2 on CO_2 capture in UiO-66(Zr) MOFs are systematically explored. The basic structure of UiO-66(Zr) is modified in each case with $-NH_2$, $-OH$, or $-Br$ functional groups, and CO_2 capture is investigated using molecular simulations. It is found that for UiO-66(Zr) with $-NH_2$ and $-OH$ groups, due to strong interactions between water and the framework, the presence of water lowers CO_2 adsorption significantly. In contrast, due to the water-phobic effects of $-Br$, and subsequent low binding strength between water and UiO-66-Br, water has much smaller effect on CO_2 capture in this MOF. Regarding SO_2 effects, the presence of SO_2 in the mixtures decreases water adsorption in both UiO-66-NH_2 and UiO-66-Br. The lower water adsorption for the $CO_2/N_2/H_2O/SO_2$ mixture in UiO-66-NH_2 can be mainly attributed to the strong binding strength between SO_2 and the framework. On the other hand, in UiO-66-Br, the lower water adsorption is mainly ascribed to the stronger affinity of water toward SO_2 rather than to the framework. The lower water adsorption makes more sites available for CO_2 adsorption, and therefore, the CO_2 adsorptions are enhanced accordingly in UiO-66-Br.

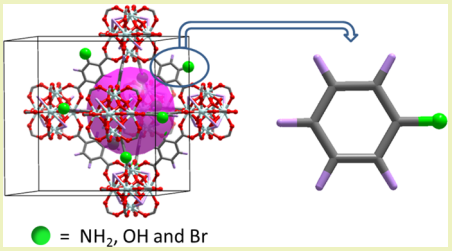

KEYWORDS: *Density functional theory, Molecular simulations, Adsorption, Separations, Selectivity*

INTRODUCTION

The flue gas emitted from coal-fired power plants includes large amounts of CO_2, leading to an increase of the global temperature. How to reduce CO_2 emissions to minimize climate change is urgently required.[1] The material, as the separation media, plays a very important role. Metal−organic frameworks (MOFs), a new class of porous solids, have been found as promising candidates in separation of various gases including CO_2.[2,3]

While the central issue in post-combustion CO_2 capture is the separation of CO_2 and N_2, the implementation of metal−organic frameworks for post-combustion CO_2 capture must take into account the fact that flue gas also includes coexisting impurities. Typically, in addition to CO_2 and N_2, the flue gas mixture also includes impurities like water, O_2, and SO_2 with corresponding concentrations of 5−7%, 3−4%, and 800 ppm, respectively.[4] In spite of the low concentrations, those impurities may significantly influence the performance of CO_2 capture in MOFs.[5,6] The adsorption of those impurities in MOFs has been studied by a couple of groups.[7−10] Recently, we investigated the effects of water on CO_2 adsorption and CO_2/N_2 separation properties in two typical MOFs with coordinatively unsaturated metal (CUM) sites: HKUST-1 and Mg-MOF-74. In HKUST-1, an increase in CO_2 adsorption was observed with an increase in hydration level as a consequence of increased binding strength between CO_2 and the hydrated framework, which is consistent with comparisons of the adsorption isotherms for the dry and hydrated 4 wt % HKUST-1 framework reported by Snurr and co-workers.[11,12] On the contrary, the presence of water decreases CO_2 adsorption in Mg-MOF-74.[13] Aside from CUMs in MOFs, the introduction of functional groups is another effective strategy to enhance the adsorption and separation ability of MOFs. Various functional groups have been employed to date for preparing MOFs for enhanced CO_2 capture performance, such as those based on nitrogen, hydroxy, nitro, halide groups, and so on.[14−20] Recently, Bell and co-workers have studied CO_2 adsorption in $(CH_3)_2$–, $(OH)_2$-, NH_2-, and COOH-functionalized MIL-53, providing detailed information about the nature and strength of the interaction between CO_2 and the framework.[21]However, how the coexisting impurities affect CO_2 adsorption and separation in MOFs depending on the properties of functional groups has been barely studied.[22]

Here, we present a systematic evaluation and comparison of the influence of impurities on CO_2 capture in UiO-66(Zr) (UiO: University of Oslo)[23] with three functional groups of $-NH_2$, $-OH$, and $-Br$. The water stability of the parent and functionalized UiO-66 has been studied by a couple of

Received: September 18, 2014
Revised: November 3, 2014
Published: November 17, 2014

groups.[24−26] It has been found that both UiO-66-NH_2 and UiO-66-Br show quite high resistance toward water and acid.[24] A large number of gas adsorption properties of UiO-66(Zr) have been explored both experimentally and computationally,[27,28] and further, the effect of functional groups on gas uptake has also been investigated.[29,30] The measurements of CO_2, CH_4, N_2, and water uptakes in amino-, nitro-, methoxy-, and naphthyl-substitued and parent UiO-66(Zr) revealed that the amino-functionalized material shows the best adsorption properties for each pure gas, which is attributed to the combination of polarity and small size of the functional group.[29] A reported computational work on the ligand functionalization effect on the CO_2/CH_4 separation performance of UiO-66(Zr) showed that UiO-66(Zr) derivatives have an enhanced affinity for CO_2 and improved CO_2/CH_4 separation abilities.[30] Therefore, in this paper, we determine the effect of impurities on the adsorption of flue gas mixtures emulating real post-combustion CO_2 streams.

COMPUTATIONAL METHODS

GCMC simulations[31] using the MUSIC code[32] were employed to calculate the adsorption of a single component and their mixtures in the MOFs. The crystal structures of UiO-66-NH_2, UiO-66-OH, and UiO-66-Br were obtained from DFT optimizations following the methods reported by Yang et al.[30] The parent UiO-66 is built up from inorganic nodes $Zr_6O_4(OH)_4$ linked with 12 terephthalate (BDC) ligands to form a three-dimensional porous structure, where each centric octahedral cage with a free diameter of 11 Å is connected with eight corner tetrahedral cages with a free diameter of 8 Å through triangular windows with a diameter of 6 Å. A schematic diagram of the UiO-66-X (X = −NH_2, −Br, and −OH) structure is given in Figure 1.

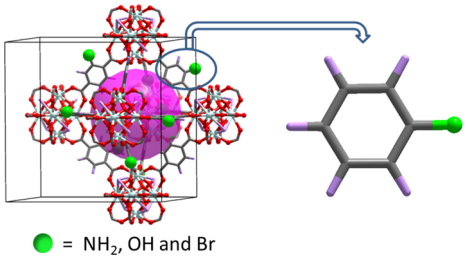

Figure 1. Schematic diagram of framework structure for UiO-66-X (left) and a structure resembling the local environment of the −X group in UiO-66-X (right). Color schemes: light turquoise = Zr, gray = C, red = O, lavender = H, and green = X.

The atomic partial charges for UiO-66-NH_2 and UiO-66-Br were taken from ref 30, and atomic partial charges for UiO-66-OH (Figure S1, Supporting Information) were calculated following the same methods reported by Yang et al.[30] In our simulations, we modeled all MOFs as rigid frameworks. A cutoff radius of 12.8 Å was applied to the Lennard−Jones (LJ) potential, and Ewald summations were used to evaluate long-range effects of the electrostatic interactions.[33] Each GCMC simulation consisted of 1×10^7 steps to guarantee equilibrium and 1×10^7 production steps.

Both CO_2 and SO_2 were represented as rigid linear triatomic molecules with one charged Lennard−Jones (LJ) interaction site located at each atom.[34,35] The geometry, potential parameters, and partial point charges for adsorbates are summarized in Table S1 of the Supporting Information. The N_2 molecule was represented as a rigid three-site model with two sites located at two N atoms and the third one located at its center of mass (COM).[34] Water was mimicked as a rigid three-site model SPC/E with one charged LJ interaction site located at each atom.[36] The LJ potential parameters for the MOF framework atoms were taken from the DREIDING[37] or UFF[38] force fields, as shown in Table S2 of the Supporting Information.[39] Lorentz−Berthelot mixing rules were employed to calculate the pair site−site interactions among the MOF framework and each gas species.

In the series of MOFs of UiO-66(Zr)-X (X = NH_2, OH, and Br), the binding energy (BE) is used to evaluate the binding strength of adsorbates (CO_2, N_2, water, and SO_2) with respect to the cluster models resembling the local environments of functional groups (−NH_2, −Br, and −OH) in MOFs. Density functional theory (DFT) calculations using the GAUSSIAN 09[40] suite of programs were employed to calculate the binding energies. The exchange and correlation functionals used for geometrical optimization were B3LYP[41] with a 6-311++G (d,p) basis set, and B97D was used for BE calculations. Compared to the popular functional B3LYP, B97D shows superiority in describing long-range dispersion interactions.[42,43] Taking UiO-66-NH_2 as an example, an aniline structure shown in Figure 1 closely resembles the local environment of the −NH_2 group in UiO-66-NH_2. The BE between CO_2 and aniline is defined as the overall energy of the following reaction.

$$CO_2 + C_6H_5NH_2 \rightarrow C_6H_5NH_2(CO_2)$$

$$=>BE = -(E_{C_6H_5NH_2(CO_2)} - E_{C_6H_5NH_2} - E_{CO_2})$$

RESULTS AND DISCUSSION

The effects of impurities including water and SO_2 were evaluated. We did not take into account the influence of oxygen in this paper because our previous results suggest negligible effects of oxygen on CO_2 capture due to the small quadrupole moment of oxygen.[11]

Effects of Water on CO_2 Capture in UiO-66(Zr)-X (X = NH_2, OH, and Br). As a first step, pure CO_2 and N_2 adsorption isotherms in UiO-66-NH_2 using DREIDING force fields were simulated and compared with the experimental results.[29] As shown in Figure S2 of the Supporting Information, simulated

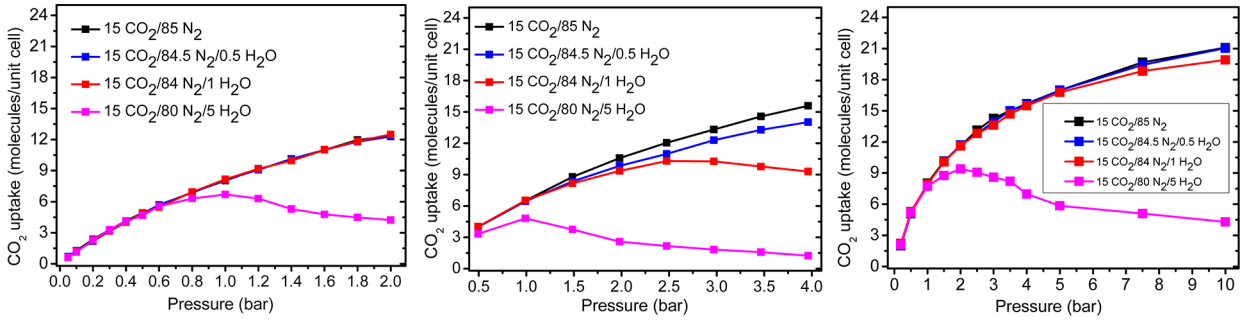

Figure 2. CO_2 uptake for $CO_2/N_2/H_2O$ mixtures with different water concentrations from 0% to 5% in UiO-66-NH_2 (left), UiO-66-OH (middle), and UiO-66-Br (right) at 298 K.

dx.doi.org/10.1021/sc500607y | ACS Sustainable Chem. Eng. 2015, 3, 117−124

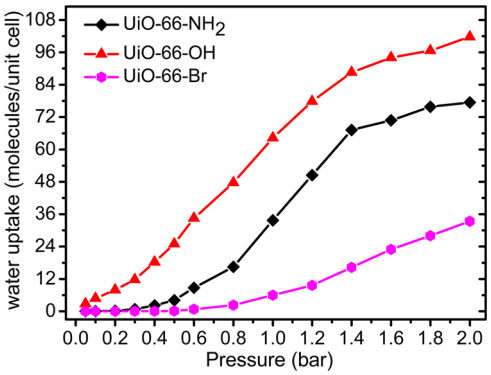

Figure 3. Water uptake for 15:80:5 $CO_2/N_2/H_2O$ mixtures in UiO-66-X (X = NH_2, OH, and Br) at 298 K.

adsorption isotherms for CO_2 and N_2 agree reasonably well with the reported experimental data. Subsequently, GCMC simulations were employed to simulate the pure CO_2 adsorption isotherms in UiO-66-OH and UiO-66-Br. CO_2 adsorption isotherms in three MOFs indicated that UiO-66-NH_2 shows the highest but UiO-66-Br shows the lowest adsorption capacity for CO_2 (Figure S3, Supporting Information).

The adsorption of a CO_2/N_2 (15:85) gas mixture (mimicking the ratio in flue gas) in UiO-66-X at 298 K was also studied with GCMC simulations, and the results are given in Figure S4 of the Supporting Information. The adsorption of CO_2 is substantially greater than N_2 in the three MOFs. The predominant CO_2 adsorption over N_2 can be attributed to the larger quadrupole moment of CO_2. Particularly, the introduction of the functional group in the framework makes CO_2 adsorption even more favorable. The separation factor of the binary mixture as a function of the total pressure was also evaluated. A slight increase in selectivity for CO_2 over N_2 is observed over the studied pressure range, which is mainly attributed to the higher CO_2 uptake at higher pressures. The calculated selectivity of CO_2 over N_2 in UiO-66-NH_2 is about ~42 at 298 K and a total pressure of 1 bar, which is comparable with the predicted selectivity for a $15CO_2/85N_2$ mixture in UiO-66-NH_2 at the same conditions obtained using both GCMC and quantitative structure−property relationship (QSPR) techniques.[44]

To examine the effect of water on the capture of CO_2 in UiO-66-X, the adsorption of $CO_2/N_2/H_2O$ mixtures with water concentrations of 0.5%, 1%, and 5% were examined. In each

Table 1. Binding Energies (BEs, kcal/mol) between Adsorbates (CO_2, N_2, Water, and SO_2) and aniline, as well as BEs between CO_2 (SO_2) and Water at B3LYP and B97D/6-311++G (d,p) with BSSE Corrected[a]

		functional	
models	optimized geometries	B3LYP	B97D
H_2O—CO_2	I	2.19	1.95
	II	1.50	1.44
$C_6H_5NH_2$—CO_2	I	1.38	3.05
	II	0.88	1.29
$C_6H_5NH_2$—N_2	I	0.42	0.95
$C_6H_5NH_2$—H_2O	I	4.89	5.72
	II	3.54	3.81
$C_6H_5NH_2$—SO_2	I	5.33	7.16
	II	1.62	2.19
H_2O—SO_2	I	3.56	4.16
	II	1.84	2.40

[a]Geometries I and II correspond to Figure 4.

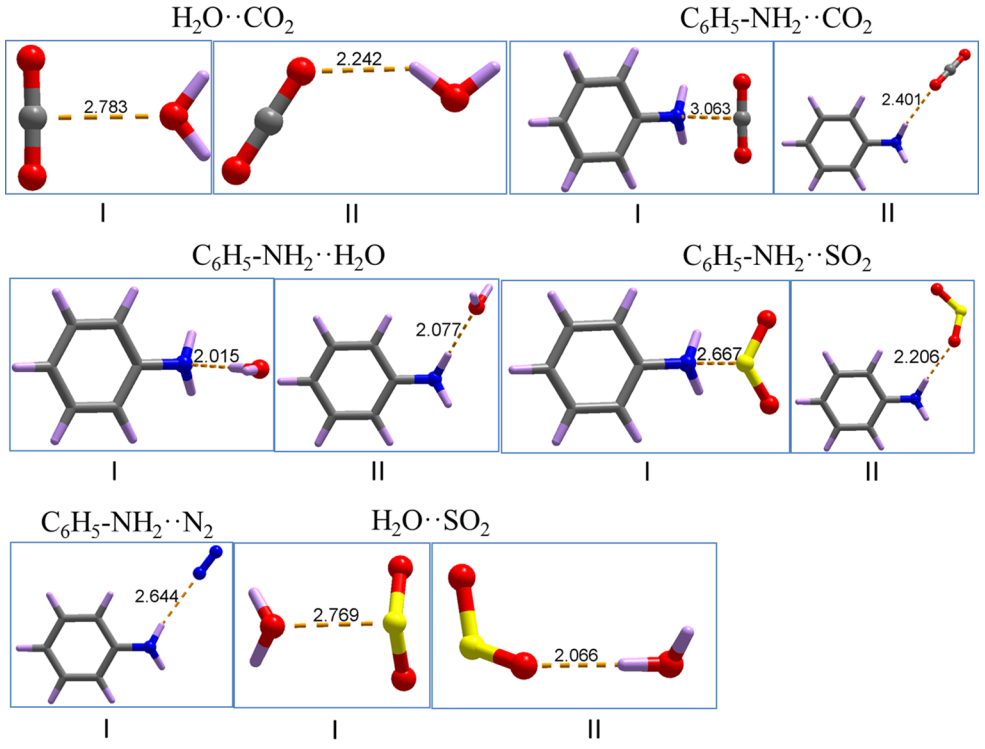

Figure 4. Optimized geometries of aniline interacting with CO_2, N_2, water, and SO_2, and water interacting with CO_2 (SO_2) at the B3LYP/6-311++G (d,p) level. Color schemes: red = O, lavender = H, blue = N, gray = C, and yellow = S.

dx.doi.org/10.1021/sc500607y | ACS Sustainable Chem. Eng. 2015, 3, 117−124

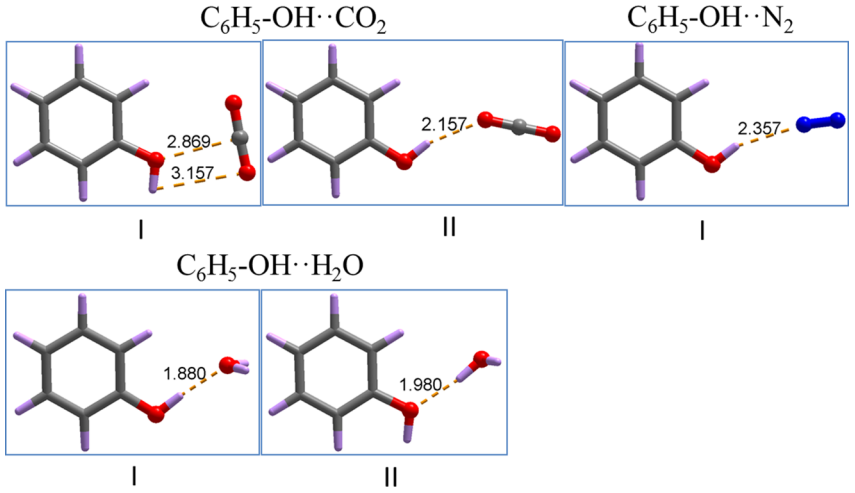

Figure 5. Optimized geometries of phenol interacting with CO_2, N_2, and water at the B3LYP/6-311++G (d,p) level. Color schemes: red = O, lavender = H, blue = N, and gray = C.

Table 2. Binding Energies (BEs, kcal/mol) between Adsorbates (CO_2, N_2, and water) and Phenol at B3LYP and B97D/6-311++G (d,p) with BSSE Corrected[a]

		functional	
models	optimized geometries	B3LYP	B97D
$C_6H_5OH—CO_2$	I	1.66	1.85
	II	1.72	1.45
$C_6H_5OH—N_2$	I	0.96	1.08
$C_6H_5OH—H_2O$	I	6.11	5.97
	II	3.74	3.79

[a]Geometries I and II correspond to Figure 5.

Table 3. Binding Energies (BEs, kcal/mol) between Adsorbates (CO_2, N_2, Water, and SO_2) and Bromobenzene at B3LYP and B97D/6-311++G (d,p) with BSSE Corrected

	functional	
models	B3LYP	B97D
$C_6H_5Br—CO_2$	0.60	1.38
$C_6H_5Br—N_2$	0.11	0.35
$C_6H_5Br—H_2O$	2.13	3.06
$C_6H_5Br—SO_2$	1.16	1.98

mixture, the water concentration varies, but the CO_2 concentration is fixed at 15%. N_2 makes up the rest of the mixture. As shown in Figure 2, the presence of water drops CO_2 uptake significantly in all of the three MOFs over the pressure range we studied, particularly for a $CO_2/N_2/H_2O$ mixture with 5% water. However, the lower extents are different depending on the properties of functional groups. For example, a substantial decrease in CO_2 adsorption was observed at a pressure lower than 1 bar in UiO-66-NH_2 and UiO-66-OH. In contrast, CO_2 uptakes for mixtures with and without water at 1 bar are almost identical in UiO-66-Br.

Figure 3 reports the water adsorption isotherms for 15:80:5 $CO_2/N_2/H_2O$ mixtures in UiO-66-X. A predominant water adsorption was observed in all of the three MOFs. The uptake of CO_2 decreases as a result of the competition of adsorption sites, as observed in Figure 2. Moreover, the comparison of water adsorption isotherms indicated that UiO-66-NH_2 and UiO-66-OH show a much higher water uptake than UiO-66-Br.

To further understand the competition behavior of all of the adsorbates (CO_2, N_2 ,and water) in UiO-66-X, DFT calculations were employed to study the binding strength of each adsorbate with the frameworks. Because aniline, phenol, and bromobenzene structures closely resemble the local environment of $-NH_2$, $-OH$, and $-BR$, the main sites for CO_2 adsorption in UiO-66-X, the binding strength between aniline (phenol and bromobenzene) and each adsorbate was evaluated. The detailed geometries and corresponding binding energies for aniline-type ligands are in Figure 4 and Table 1. The same information for phenol-type ligands is in Figure 5 and Table 2 and for bromobenzene-type ligands is in Figure 6 and Table 3. As listed in Table 1, water shows the highest affinity among CO_2, N_2, and water toward aniline through either N or H sites in geometry 1 and geometry II. Two binding sites were also identified for CO_2 with corresponding binding energies of 3.05 and 1.29 kcal/mol. N_2 shows the lowest binding strength toward aniline. Due to the higher binding energy between water and UiO-66-NH_2, the presence of water decreases both the adsorption of CO_2 and N_2. This is

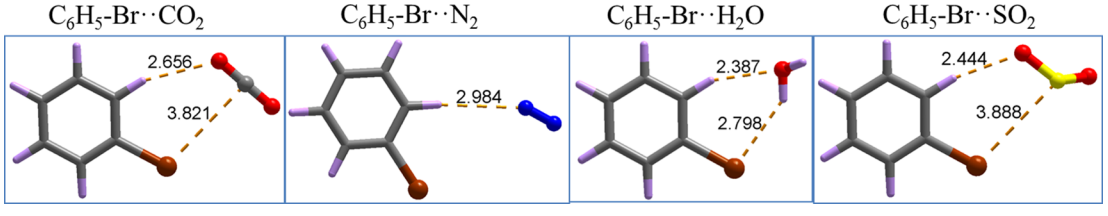

Figure 6. Optimized geometries of C_6H_5Br interacting with CO_2, N_2, water, and SO_2 at the B3LYP/6-311++G (d,p) level. Color schemes: red = O, lavender = H, brown = Br, blue = N, gray = C, and yellow = S.

dx.doi.org/10.1021/sc500607y | ACS Sustainable Chem. Eng. 2015, 3, 117−124

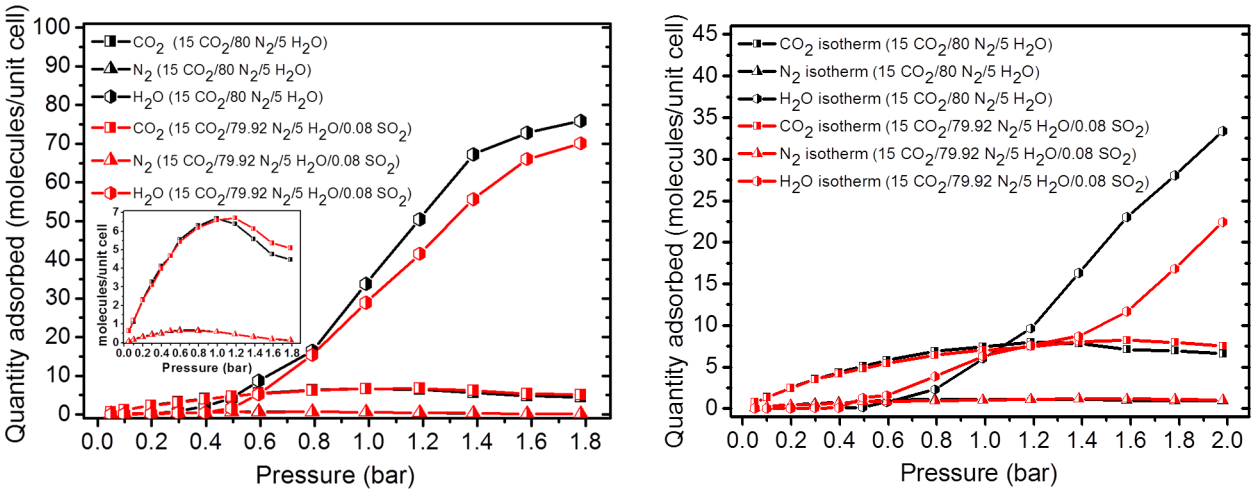

Figure 7. Simulated CO_2, N_2, and water isotherms for a $CO_2/N_2/H_2O/SO_2$ mixture and a $CO_2/N_2/H_2O$ mixture in UiO-66-NH_2 (left) and UiO-66-Br (right) at 298 K.

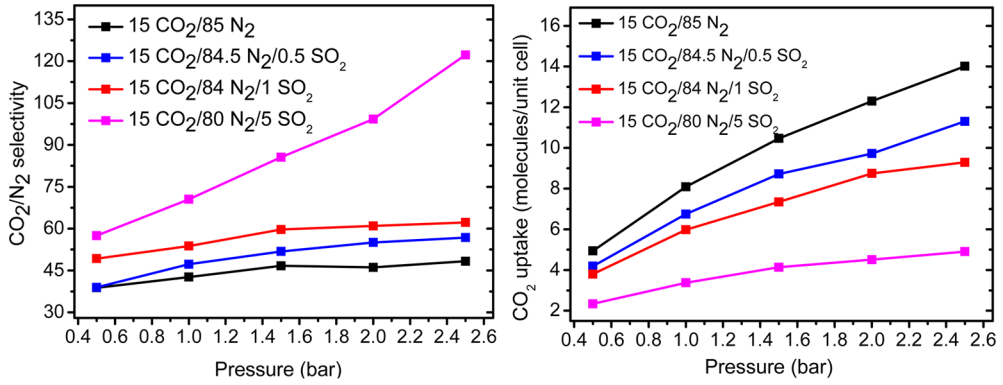

Figure 8. Simulated CO_2/N_2 selectivity (left) and CO_2 uptake (right) for $CO_2/N_2/SO_2$ mixtures with different SO_2 concentrations from 0% to 5% in UiO-66-NH_2 at 298 K.

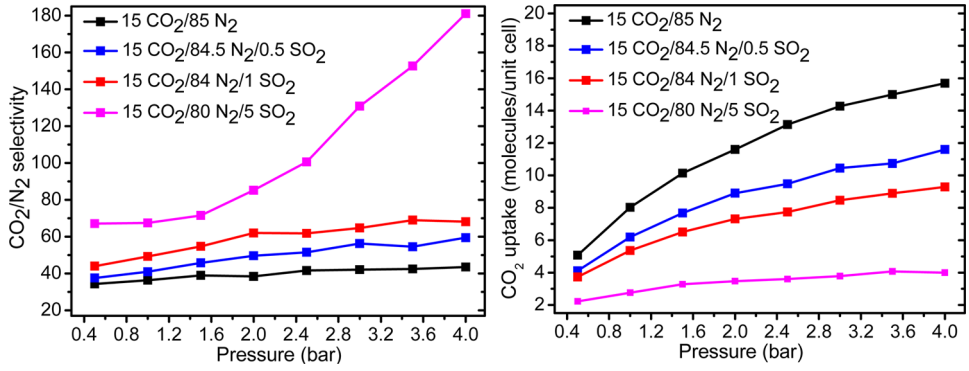

Figure 9. Simulated CO_2/N_2 selectivity (left) and CO_2 uptake (right) for $CO_2/N_2/SO_2$ mixtures with different SO_2 concentrations from 0% to 5% in UiO-66-Br at 298 K.

consistent with the fact that the adsorption of CO_2 decreases for $CO_2/N_2/H_2O$ mixtures. The strong adsorption of water on the aniline-type ligand indicated that the removal of water from flue gas or at least partial removal is essential for large-scale application of amine-functionalized MOFs on CO_2 capture.

For phenol-type ligands, water shows the highest affinity toward phenol as well through either H or O sites. Two binding geometries were also identified for CO_2 with corresponding binding energies of 1.85 and 1.45 kcal/mol. N_2 shows the lowest binding strength toward phenol. Similar with $CO_2/N_2/H_2O$ adsorption in UiO-66-NH_2, due to the higher binding energy between water and UiO-66-OH, the presence of water decreases the adsorption of CO_2. This is also consistent with the lower CO_2 uptake for $CO_2/N_2/H_2O$ mixtures shown in Figure 2. The strong adsorption of water on the phenol-type ligand indicated that the removal of water from the flue gas or at least partial removal is also essential for large-scale application of hydroxyl functionalized MOFs on CO_2 capture.

In contrast, due to the water-phobic effect of −Br, the binding energy between water and bromobenzene is only 3.06

dx.doi.org/10.1021/sc500607y | ACS Sustainable Chem. Eng. 2015, 3, 117−124

kcal/mol (Figure 6), which is much smaller than those between water and aniline and water and phenol. Therefore, different from water effects in UiO-66-NH_2 and UiO-66-OH, where significant water molecules are adsorbed in the frameworks thus leading to a decrease in adsorption of both CO_2 and N_2 at relatively lower pressures, water effects on CO_2 capture in UiO-66-Br are much smaller.

Effects of SO_2 on CO_2 Capture in UiO-66(Zr)-X (X = NH_2 and Br). To study the effect of SO_2 on CO_2 capture in UiO-66-X, two cases were considered. First, we studied the SO_2 effects on the capture of CO_2 in UiO-66-X for a $CO_2/N_2/H_2O/SO_2$ mixture (mimicking the ratio of the flue gas)[4] with a bulk composition of 15:79.92:5:0.08. The results were compared with those for a 15:80:5 $CO_2/N_2/H_2O$ mixture without SO_2. Second, CO_2 capture in the UiO-66-X for $CO_2/N_2/SO_2$ mixtures with different concentrations of SO_2 were explored. Depending on the source of coal and combustion conditions, the concentrations of the SO_2 in flue gas may be different. Therefore, the investigation of adsorption of flue gas mixtures with various SO_2 concentrations is necessary.

For the first case, Figure 7 compares the adsorption isotherms of CO_2, N_2, and water for two mixtures in both UiO-66-NH_2 and UiO-66-Br. One interesting result from these comparisons is that even with trace amounts of SO_2 in the mixture, water adsorption drops significantly in both MOFs. Meanwhile, CO_2 uptake increases slightly for the 15:79.92:5:0.08 $CO_2/N_2/H_2O/SO_2$ mixture in UiO-66-Br.

To investigate why the presence of SO_2 lowers water adsorption but improves CO_2 adsorption, DFT calculations were employed to evaluate the binding strength of each adsorbate including CO_2, N_2, SO_2, and water in both MOFs. For the MOF modified with $-NH_2$, the binding energy between SO_2 and aniline is as high as 7.16 kcal/mol, which is the highest among all adsorbates. The largest binding energy indicated the strongest affinity of SO_2 to the framework. Therefore, when SO_2 is present in the mixture, it competes with water for the amine sites thus decreasing the adsorption of water. On the other hand, for the MOF modified with −Br, SO_2 only shows weak interaction with bromobenzene (Table 3). This indicates that the competition of adsorption sites by SO_2 could not be the main contribution to the significant decrease in water adsorption. However, because water shows a stronger affinity toward SO_2 than the framework, water prefers to interact with SO_2 in flue gas. Therefore, the presence of SO_2 in the mixture decreases the water uptake in the framework. The reduced water adsorption in the framework makes more sites available for adsorption of other molecules. Because the SO_2 concentration is very low and most of the SO_2 molecules interact with either the framework or water molecules, there are many more chances for CO_2 to occupy those available sites. The CO_2 uptake is enhanced accordingly. This is in fact what we observed in Figure 7, where higher CO_2 uptake was observed for the $CO_2/N_2/H_2O/SO_2$ mixture in UiO-66-Br. Due to larger amounts of SO_2 present at higher pressures, SO_2 effects are more obvious.

For the second case, Figures 8 and 9 report the selectivity of CO_2 over N_2 and CO_2 uptake for $CO_2/N_2/SO_2$ mixtures with SO_2 concentrations of 0%, 0.5%, 1%, and 5% in UiO-66-NH_2 and UiO-66-Br. The results show that as the SO_2 concentration increases in the mixture, CO_2 uptake drops significantly in both MOFs. This is expected due to a much stronger interaction between SO_2 and both frameworks than CO_2.

CONCLUSIONS

In this study, the influences of water and SO_2 on CO_2 adsorption and separation in UiO-66(Zr) MOFs with functional groups of $-NH_2$, −OH, and −Br were evaluated using a combination of GCMC and DFT simulations. We found that in these MOFs CO_2 uptake is substantially greater than N_2 for the CO_2/N_2 mixture adsorption. Due to a stronger adsorption of water on the phenol and aniline-type ligands, the impact of water on CO_2 adsorption and CO_2/N_2 separation in ones with $-NH_2$ and −OH groups is much higher. In contrast, because of the hydrophobic property of −Br causing a low binding strength between water and the framework, water shows much smaller effects on CO_2 capture in UiO-66-Br. In terms of SO_2 effects, it was found that the presence of SO_2 in the mixtures decreases water adsorption in both UiO-66-NH_2 and UiO-66-Br, although the associated reasons are different. The lower water adsorption for the $CO_2/N_2/H_2O/SO_2$ mixture in UiO-66-NH_2 can be mainly attributed to the stronger binding between SO_2 and the framework. However, in UiO-66-Br, because water would rather interact with SO_2 than interact with the framework, the presence of SO_2 decreases water adsorption in the MOF. The lower water adsorption makes more sites available for CO_2; accordingly, the CO_2 uptake is enhanced in UiO-66-Br.

ASSOCIATED CONTENT

Supporting Information

DFT atomic partial charges for the UiO-66-OH structure (Figure S1). GCMC simulated adsorption isotherms and comparison with experimental data of CO_2 and N_2 at 298 K in UiO-66-NH_2 (Figure S2). GCMC simulated CO_2 adsorption isotherm in UiO-66-OH compared with UiO-66-NH_2 and UiO-66-Br at 298 K (Figure S3). GCMC adsorption isotherms and selectivity of CO_2 over N_2 for a 15:85 CO_2/N_2 mixture in UiO-66-NH_2, UiO-66-OH, and UiO-66-Br at 298 K (Figure S4). Force field parameters of adsorbates and for MOF atoms (Table S1 and S2). This material is available free of charge via the Internet at http://pubs.acs.org.

AUTHOR INFORMATION

Corresponding Author

*E-mail: balbuena@tamu.edu.

Notes

The authors declare no competing financial interest.

ACKNOWLEDGMENTS

We are thankful for the financial support from ARPA-E through the IMPACCT program (AR0000073). Computational resources from the Texas A&M Supercomputing Facilities and Texas A&M University Brazos HPC cluster are gratefully acknowledged.

REFERENCES

(1) Rochelle, G. T. Amine scrubbing for CO_2 capture. *Science* **2009**, *325*, 1652−1654.

(2) Li, J. R.; Ma, Y. G.; McCarthy, M. C.; Sculley, J.; Yu, J. M.; Jeong, H. K.; Balbuena, P. B.; Zhou, H. C. Carbon dioxide capture-related gas adsorption and separation in metal-organic frameworks. *Coord. Chem. Rev.* **2011**, *255*, 1791−1823.

(3) Bae, Y. S.; Snurr, R. Q. Development and evaluation of porous materials for carbon dioxide separation and capture. *Angew. Chem., Int. Ed.* **2011**, *50*, 11586−11596.

(4) Granite, E. J.; Pennline, H. W. Photochemical removal of mercury from flue gas. *Ind. Eng. Chem. Res.* **2002**, *41*, 5470−5476.
(5) Babarao, R.; Jiang, J. W. Upgrade of natural gas in rho zeolite-like metal-organic framework and effect of water: A computational study. *Energy Environ. Sci.* **2009**, *2*, 1088−1093.
(6) Ding, L. F.; Yazaydin, A. O. How well do metal-organic frameworks tolerate flue gas impurities? *J. Phys. Chem. C* **2012**, *116*, 22987−22991.
(7) Thallapally, P. K.; Motkuri, R. K.; Fernandez, C. A.; McGrail, B. P.; Behrooz, G. S. Prussian blue analogues for CO_2 and SO_2 capture and separation applications. *Inorg. Chem.* **2010**, *49*, 4909−4915.
(8) Burtch, N. C.; Jasuja, H.; Walton, K. S. Water stability and adsorption in metal-organic frameworks. *Chem. Rev.* **2014**, *114*, 10575−612.
(9) Huang, H. L.; Zhang, W. J.; Liu, D. H.; Zhong, C. L. Understanding the effect of trace amount of water on CO_2 capture in natural gas upgrading in metal−organic frameworks: A molecular simulation study. *Ind. Eng. Chem. Res.* **2012**, *51*, 10031−10038.
(10) Fernandez, C. A.; Thallapally, P. K.; Motkuri, R. K.; Nune, S. K.; Sumrak, J. C.; Tian, J.; Liu, J. Gas-induced expansion and contraction of a fluorinated metal-organic framework. *Cryst. Growth Des.* **2010**, *10*, 1037−1039.
(11) Yu, J. M.; Ma, Y. G.; Balbuena, P. B. Evaluation of the impact of H_2O, O_2, and SO_2 on postcombustion CO_2 capture in metal−organic frameworks. *Langmuir* **2012**, *28*, 8064−8071.
(12) Yazaydin, A. O.; Benin, A. I.; Faheem, S. A.; Jakubczak, P.; Low, J. J.; Willis, R. R.; Snurr, R. Q. Enhanced CO_2 adsorption in meta−organic frameworks via occupation of open-metal sites by coordinated water molecules. *Chem. Mater.* **2009**, *21*, 1425−1430.
(13) Yu, J.; Balbuena, P. B. Water effects on post-combustion CO_2 capture in Mg-MOF-74. *J. Phys. Chem. C* **2013**, *117*, 3383−3388.
(14) Phan, A.; Doonan, C. J.; Uribe-Romo, F. J.; Knobler, C. B.; O'Keeffe, M.; Yaghi, O. M. Synthesis, structure, and carbon dioxide capture properties of zeolitic imidazolate frameworks. *Acc. Chem. Res.* **2009**, *43*, 58−67.
(15) Gadzikwa, T.; Farha, O. K.; Mulfort, K. L.; Hupp, J. T.; Nguyen, S. T. A Zn-based, pillared paddlewheel MOF containing free carboxylic acids via covalent post-synthesis elaboration. *Chem. Commun.* **2009**, 3720−3722.
(16) Inubushi, Y.; Horike, S.; Fukushima, T.; Akiyama, G.; Matsuda, R.; Kitagawa, S. Modification of flexible part in Cu^{2+} interdigitated framework for CH_4/CO_2 separation. *Chem. Commun.* **2010**, *46*, 9229−9231.
(17) Tian, Y.-Q.; Yao, S.-Y.; Gu, D.; Cui, K.-H.; Guo, D.-W.; Zhang, G.; Chen, Z.-X.; Zhao, D.-Y. Cadmium imidazolate frameworks with polymorphism, high thermal stability, and a large surface area. *Chem.—Eur. J.* **2010**, *16*, 1137−1141.
(18) Tan, Y.-X.; Wang, F.; Kang, Y.; Zhang, J. Dynamic microporous indium(iii)-4,4[prime or minute]-oxybis(benzoate) framework with high selectivity for the adsorption of CO_2 over N_2. *Chem. Commun.* **2011**, *47*, 770−772.
(19) Liang, J.; Shimizu, G. K. H. Crystalline zinc diphosphonate metal−organic framework with three-dimensional microporosity. *Inorg. Chem.* **2007**, *46*, 10449−10451.
(20) Neofotistou, E.; D. Malliakas, C.; N. Trikalitis, P. Unprecedented sulfone-functionalized metal−organic frameworks and gas-sorption properties. *Chem.—Eur. J.* **2009**, *15*, 4523−4527.
(21) Torrisi, A.; Bell, R. G.; Mellot-Draznieks, C. Predicting the impact of functionalized ligands on CO_2 adsorption in MOFs: A combined DFT and grand canonical Monte Carlo study. *Microporous Mesoporous Mater.* **2013**, *168*, 225−238.
(22) Chen, Y. F.; Jiang, J. W. A bio-metal-organic framework for highly selective CO_2 capture: A molecular simulation study. *ChemSusChem.* **2010**, *3*, 982−988.
(23) Cavka, J. H.; Jakobsen, S.; Olsbye, U.; Guillou, N.; Lamberti, C.; Bordiga, S.; Lillerud, K. P. A new zirconium inorganic building brick forming metal organic frameworks with exceptional stability. *J. Am. Chem. Soc.* **2008**, *130*, 13850−13851.
(24) Kandiah, M.; Nilsen, M. H.; Usseglio, S.; Jakobsen, S.; Olsbye, U.; Tilset, M.; Larabi, C.; Quadrelli, E. A.; Bonino, F.; Lillerud, K. P. Synthesis and stability of tagged UiO-66 Zr-MOFs. *Chem. Mater.* **2010**, *22*, 6632−6640.
(25) DeCoste, J. B.; Peterson, G. W.; Jasuja, H.; Glover, T. G.; Huang, Y. G.; Walton, K. S. Stability and degradation mechanisms of metal-organic frameworks containing the $Zr_6O_4(OH)(4)$ secondary building unit. *J. Mater. Chem. A* **2013**, *1*, 5642−5650.
(26) DeCoste, J. B.; Peterson, G. W.; Schindler, B. J.; Killops, K. L.; Browe, M. A.; Mahle, J. J. The effect of water adsorption on the structure of the carboxylate containing metal-organic frameworks Cu-BTC, Mg-MOF-74, and UiO-66. *J. Mater. Chem. A* **2013**, *1*, 11922−11932.
(27) Yang, Q.; Wiersum, A. D.; Jobic, H.; Guillerm, V.; Serre, C.; Llewellyn, P. L.; Maurin, G. Understanding the thermodynamic and kinetic behavior of the CO_2/CH_4 gas mixture within the porous zirconium terephthalate UiO-66(Zr): A joint experimental and modeling approach. *J. Phys. Chem. C* **2011**, *115*, 13768−13774.
(28) Yang, Q.; Jobic, H.; Salles, F.; Kolokolov, D.; Guillerm, V.; Serre, C.; Maurin, G. Probing the dynamics of CO_2 and CH_4 within the porous zirconium terephthalate UiO-66(Zr): A synergic combination of neutron scattering measurements and molecular simulations. *Chem.—Eur. J.* **2011**, *17*, 8882−8889.
(29) Cmarik, G. E.; Kim, M.; Cohen, S. M.; Walton, K. S. Tuning the adsorption properties of UiO-66 via ligand functionalization. *Langmuir* **2012**, *28*, 15606−15613.
(30) Yang, Q.; Wiersum, A. D.; Llewellyn, P. L.; Guillerm, V.; Serre, C.; Maurin, G. Functionalizing porous zirconium terephthalate UiO-66(Zr) for natural gas upgrading: A computational exploration. *Chem. Commun.* **2011**, *47*, 9603−9605.
(31) Allen, M. P.; Tildesley, D. J.: *Computer Simulation of Liquids*; Oxford University Press; Oxford, U.K.,1987.
(32) Gupta, A.; Chempath, S.; Sanborn, M. J.; Clark, L. A.; Snurr, R. Q. Object-oriented programming paradigms for molecular modeling. *Mol. Simul.* **2003**, *29*, 29−46.
(33) Deleeuw, S. W.; Perram, J. W.; Smith, E. R. Simulation of electrostatic systems in periodic boundary-conditions 0.1. Lattice sums and dielectric-constants. *Proc. R. Soc. A* **1980**, *373*, 27−56.
(34) Potoff, J. J.; Siepmann, J. I. Vapor−liquid equilibria of mixtures containing alkanes, carbon dioxide, and nitrogen. *AIChE J.* **2001**, *47*, 1676−1682.
(35) Sokolic, F.; Guissani, Y.; Guillot, B. Molecular-dynamics simulations of thermodynamic and structural−properties of liquid SO_2. *Mol. Phys.* **1985**, *56*, 239−253.
(36) Berendsen, H. J. C.; Grigera, J. R.; Straatsma, T. P. The missing term in effective pair potentials. *J. Phys. Chem.* **1987**, *91*, 6269−6271.
(37) Mayo, S. L.; Olafson, B. D.; Goddard, W. A. DREIDING − A generic force-field for molecular simulations. *J. Phys. Chem.* **1990**, *94*, 8897−8909.
(38) Rappe, A. K.; Casewit, C. J.; Colwell, K. S.; Goddard, W. A.; Skiff, W. M. UFF, a full periodic-table force-field for molecular mechanics and molecular-dynamics simulations. *J. Am. Chem. Soc.* **1992**, *114*, 10024−10035.
(39) Yang, Q. Y.; Wiersum, A. D.; Llewellyn, P. L.; Guillerm, V.; Serred, C.; Maurin, G. Functionalizing porous zirconium terephthalate UiO-66(Zr) for natural gas upgrading: A computational exploration. *Chem. Commun.* **2011**, *47*, 9603−9605.
(40) Frisch, M. J.; Trucks, G. W.; Schlegel, H. B.; Scuseria, G. E.; Robb, M. A.; Cheeseman, J. R.; Scalmani, G.; Barone, V.; Mennucci, B.; Petersson, G. A.; Nakatsuji, H.; Caricato, M.; Li, X.; Hratchian, H. P.; Izmaylov, A. F.; Bloino, J.; Zheng, G.; Sonnenberg, J. L.; Hada, M.; Ehara, M.; Toyota, K.; Fukuda, R.; Hasegawa, J.; Ishida, M.; Nakajima, T.; Honda, Y.; Kitao, O.; Nakai, H.; Vreven, T.; Montgomery, J. A., Jr.; Peralta, P. E.; Ogliaro, F.; Bearpark, M.; Heyd, J. J.; Brothers, E.; Kudin, K. N.; Staroverov, V. N.; Kobayashi, R.; Normand, J.; Raghavachari, K.; Rendell, A.; Burant, J. C.; Iyengar, S. S.; Tomasi, J.; Cossi, M.; Rega, N.; Millam, N. J.; Klene, M.; Knox, J. E.; Cross, J. B.; Bakken, V.; Adamo, C.; Jaramillo, J.; Gomperts, R.; Stratmann, R. E.; Yazyev, O.; Austin, A. J.; Cammi, R.; Pomelli, C.; Ochterski, J. W.;

Martin, R. L.; Morokuma, K.; Zakrzewski, V. G.; Voth, G. A.; Salvador, P.; Dannenberg, J. J.; Dapprich, S.; Daniels, A. D.; Farkas, Ö.; Ortiz, J. V.; Cioslowski, J.; Fox, D. J. *Gaussian 09*, revision A.08 ; Gaussian, Inc.: Wallingford, CT, 2009.

(41) Becke, A. D. Density-functional exchange-energy approximation with correct asymptotic-behavior. *Phys. Rev. A* **1988**, *38*, 3098−3100.

(42) Plumley, J. A.; Dannenberg, J. J. A comparison of the behavior of functional/basis set combinations for hydrogen-bonding in the water dimer with emphasis on basis set superposition error. *J. Comput. Chem.* **2011**, *32*, 1519−1527.

(43) Burns, L. A.; Vazquez-Mayagoitia, A.; Sumpter, B. G.; Sherrill, C. D. Density-functional approaches to noncovalent interactions: A comparison of dispersion corrections (DFT-D), exchange-hole dipole moment (XDM) theory, and specialized functionals. *J. Chem. Phys.* **2011**, 134.

(44) Wu, D.; Yang, Q. Y.; Zhong, C. L.; Liu, D. H.; Huang, H. L.; Zhang, W. J.; Maurin, G. Revealing the structure−property relationships of metal−organic frameworks for CO_2 capture from flue gas. *Langmuir* **2012**, *28*, 12094−12099.